Electronic Supplementary Material (ESI) for Dalton Transactions.
This journal is © The Royal Society of Chemistry 2023

Controlled synthesis of Cr_x-$FeCo_2P$ nanoarrays on nickel foam for overall urea splitting

Xinyu Li[a], Yanhong Wang[a], Xiaoqiang Du[a*] and Xiaoshuang Zhang[b]

[a] School of Chemistry and Chemical Engineering, Shanxi Key Laboratory of High Performance Battery Materials and Devices, North University of China, Xueyuan road 3, Taiyuan 030051, People's Republic of China. E-mail: duxq16@nuc.edu.cn

[b] School of Environment and Safety Engineering, North University of China, Xueyuan road 3, Taiyuan 030051, People's Republic of China.

Materials and chemicals

Concentrated hydrochloric acid (HCl, 12 mol/L), acetone ($CO(CH_3)_2$, >99%), Cobalt nitrate hexahydrate ($Co(NO_3)_2·6H_2O$, >99%), Chromic nitrate nonahydrate($Cr(NO_3)_3·9H_2O$, >99%), Ferric nitrate nonahydrate($Fe(NO_3)_3·9H_2O$, >99%) Ammonium fluoride (NH_4F, >99%), urea ($CO(NH_2)_2$, >99%) and potassium hydroxide (KOH, >99%) were purchased from Sinopharm Chemical Reagent Ltd and could be used directly without further purification. Nickel foam (NF, 1.0 mm in thickness) was served as substrates of target catalysts with pretreatment before use. Furthermore, sufficient ultrapure water was prepared throughout the experiments.

DFT computation details: The DFT calculations were performed using the Cambridge Sequential Total Energy Package (CASTEP) with the plane-wave pseudo-potential method. The geometrical structures of the (020) plane of $Cr_{0.1}$-$FeCo_2P$ and $FeCo_2P$ was optimized by the generalized gradient approximation (GGA) methods. The Revised Perdew-Burke-Ernzerh of (RPBE) functional was used to treat the electron exchange correlation interactions. A Monkhorst Pack grid k-points of 5*6*1 of $Cr_{0.1}$-$FeCo_2P$ and $FeCo_2P$, a plane-wave basis set cut-off energy of 500 eV were used for integration of the Brillouin zone. The structures were optimized for energy and force convergence set at 0.05 eV/A and 2.0×10^{-5} eV, respectively. The Gibbs free energy of H adsorption was calculated as follows:

$$\Delta G_{H^*} = \Delta E_{H^*} + \Delta ZPE - T\Delta S$$

Where ΔZPE is the zero-point energy and TΔS stands for the entropy corrections. According to the previous report by Norskov et al., we used the 0.24 eV for the ΔZPE - TΔS of hydrogen

adsorption in this work.

Res: J. Electrochem. Soc., **2005**, 152, J23.

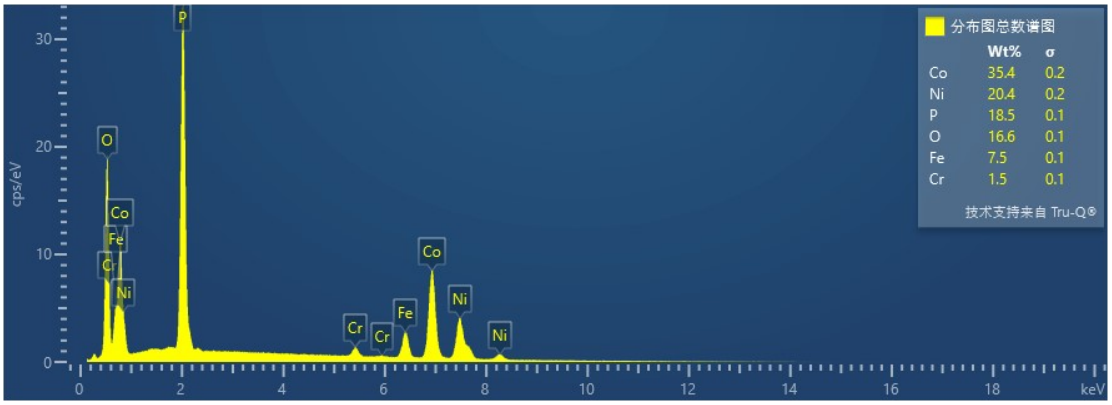

Fig. S1 EDS spectra of the $Cr_{0.1}$-$FeCo_2P$/NF material.

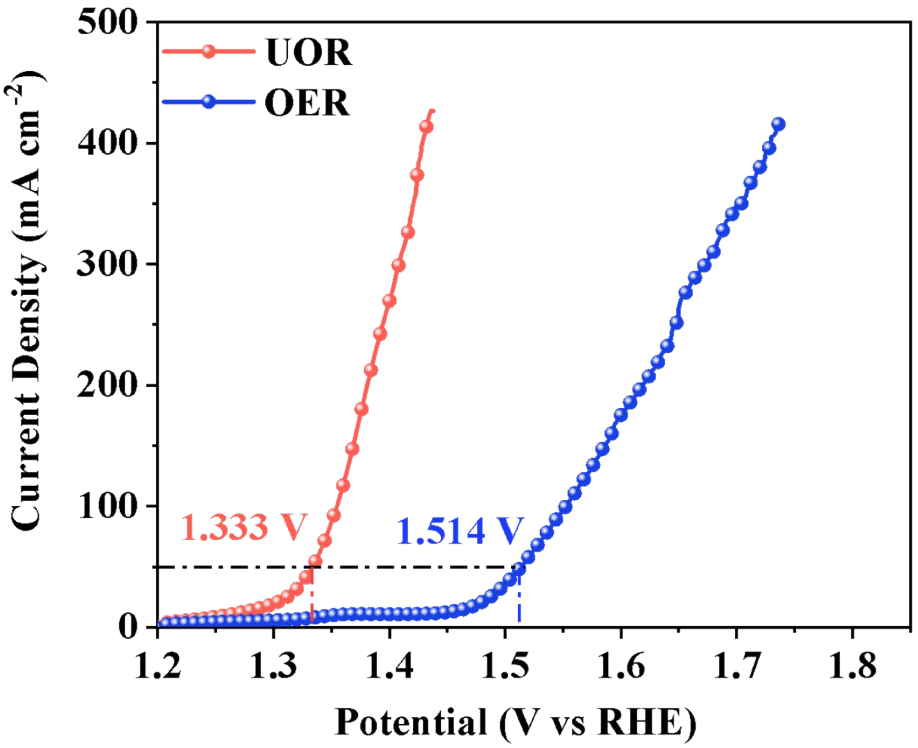

Fig. S2 Comparison of potentials of UOR and OER.

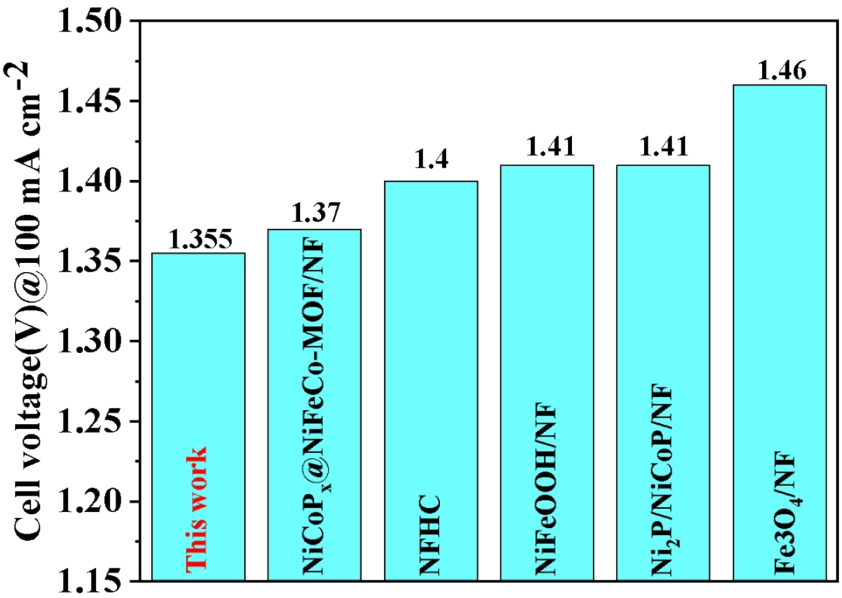

Fig. S3 Comparison of urea electrolysis UOR performance with previously reported electrocatalysts[1-5].

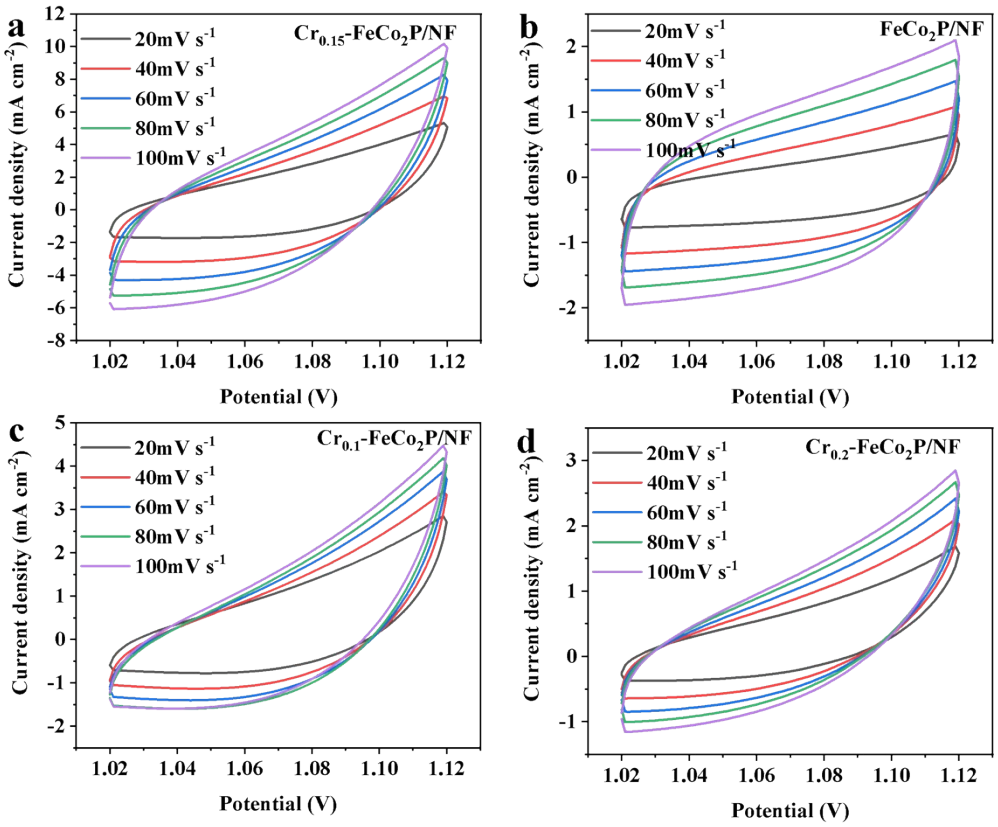

Fig. S4 In 1.0 M KOH + 0. 5M urea, cyclic voltammograms of a) $Cr_{0.15}$-$FeCo_2P$/NF, b) $FeCo_2P$/NF, c) $Cr_{0.1}$-$FeCo_2P$/NF and d) $Cr_{0.2}$-$FeCo_2P$/NF at the different scan rates varying from 20 to 100 $mV \cdot s^{-1}$ for UOR.

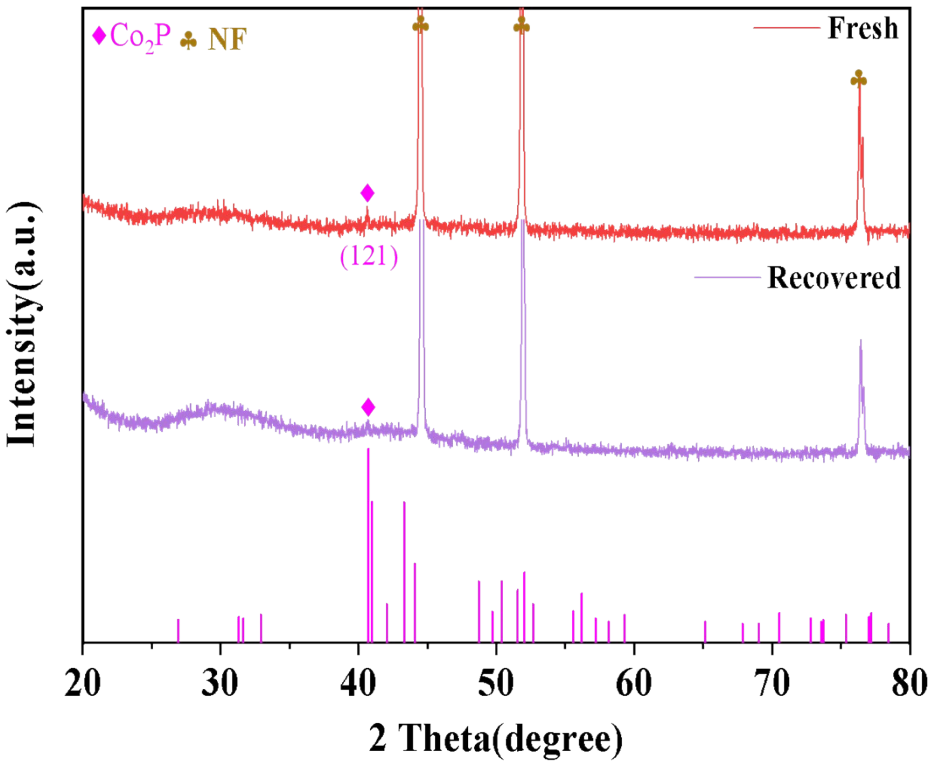

Fig. S5 XRD patterns before and after OER@$Cr_{0.15}$-$FeCo_2P$/NF after 12 h.

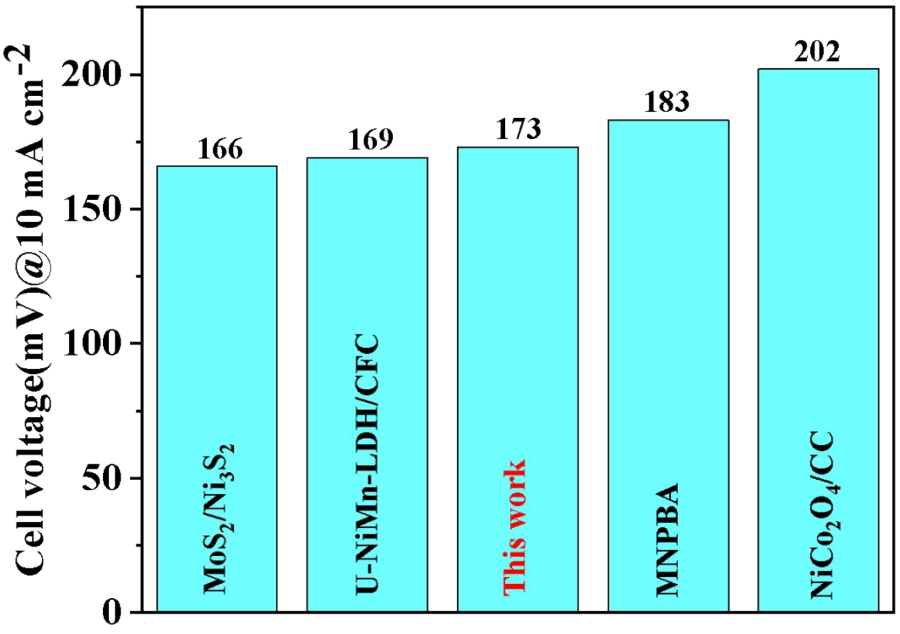

Fig. S6 Comparison of urea electrolysis HER performance with previously reported electrocatalysts[6-9].

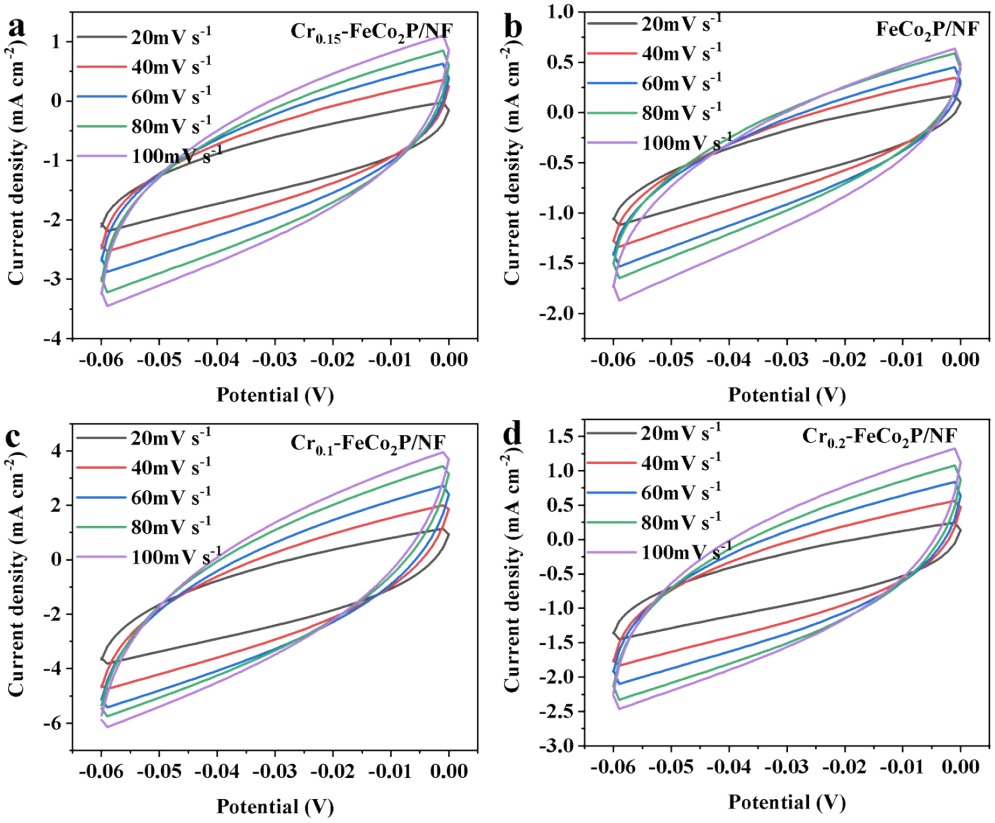

Fig. S7 In 1.0 M KOH + 0. 5M urea, cyclic voltammograms of a) $Cr_{0.15}$-$FeCo_2P$/NF, b) $FeCo_2P$/NF, c) $Cr_{0.1}$-$FeCo_2P$/NF and d) $Cr_{0.2}$-$FeCo_2P$/NF at the different scan rates varying from 20 to 100 $mV \cdot s^{-1}$ for HER.

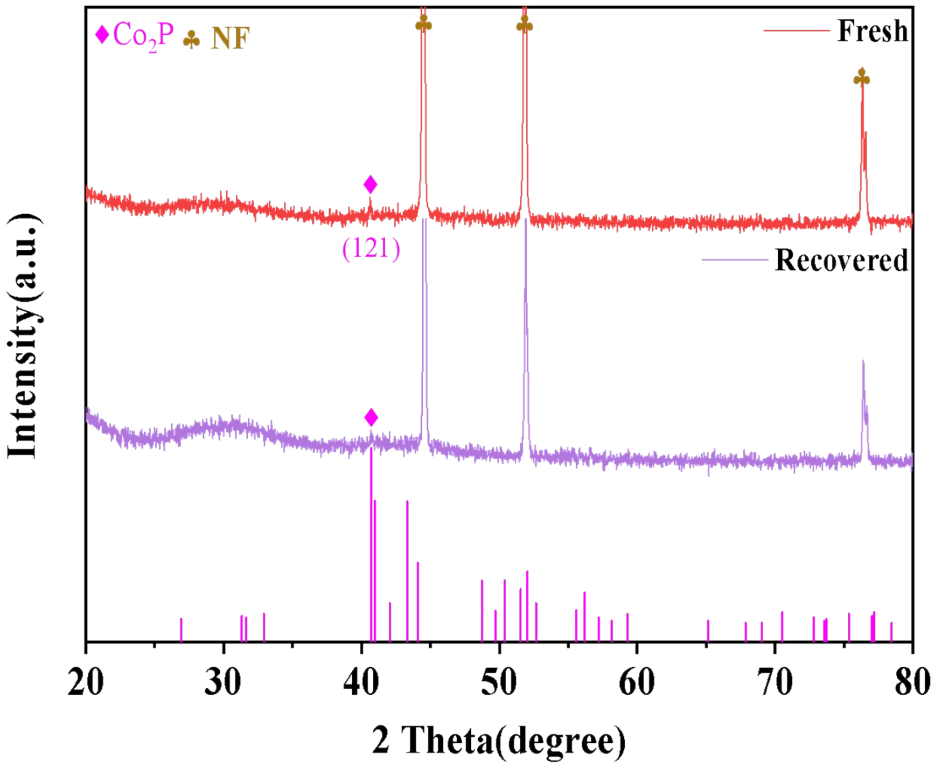

Fig. S8 XRD patterns before and after HER@$Cr_{0.1}$-$FeCo_2P$/NF after 12 h.

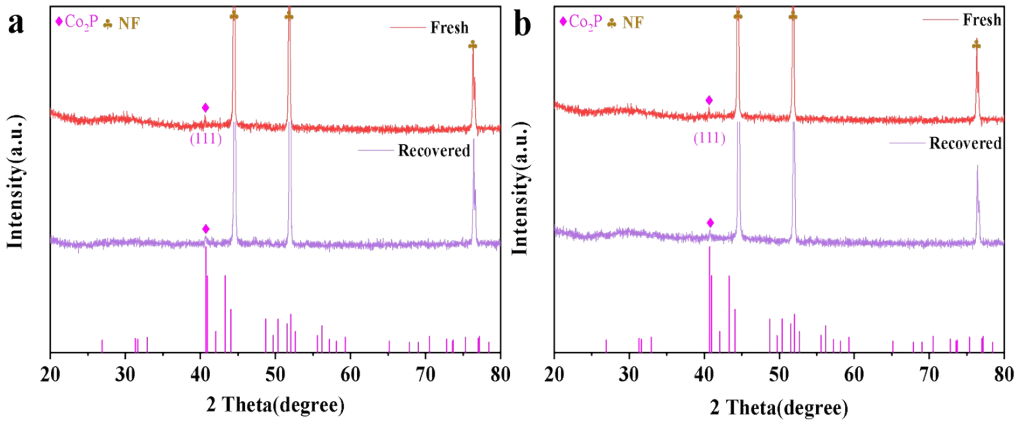

Fig. S9 XRD diagram of $Cr_{0.15}$-$FeCo_2P$/NF//$Cr_{0.1}$-$FeCo_2P$/NF before and after 12 h for overall urea electrolysis, anode (a) and cathode (b).

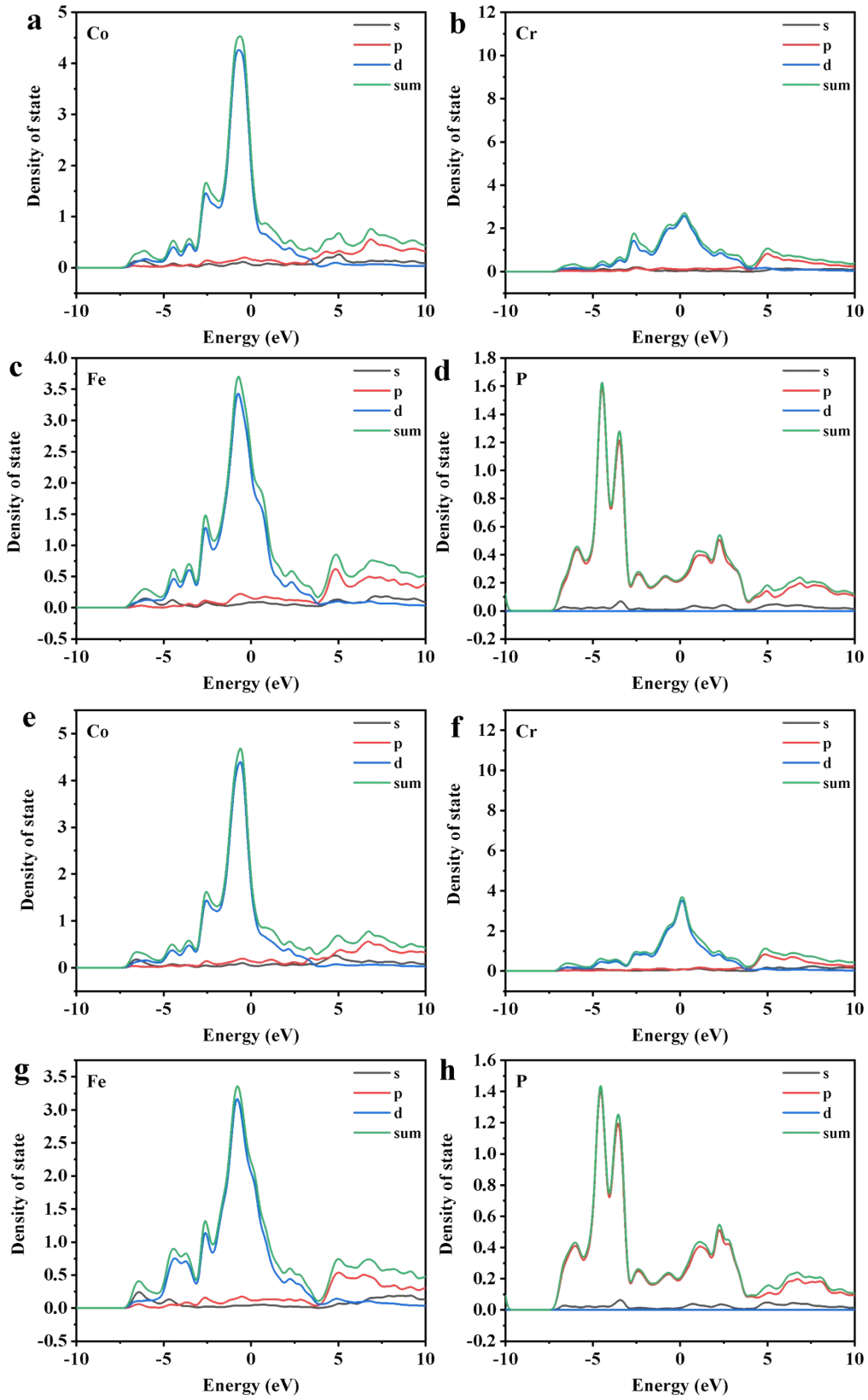

Fig. S10 The partial density of states, (a) Co , (b) Cr, (c) Fe and (b) P for the Cr-$FeCo_2P$-$Cr_{1\text{-Site}}$; (e) Co , (f) Cr, (g) Fe and (h) P for the Cr-$FeCo_2P$-$Cr_{2\text{-Site}}$.

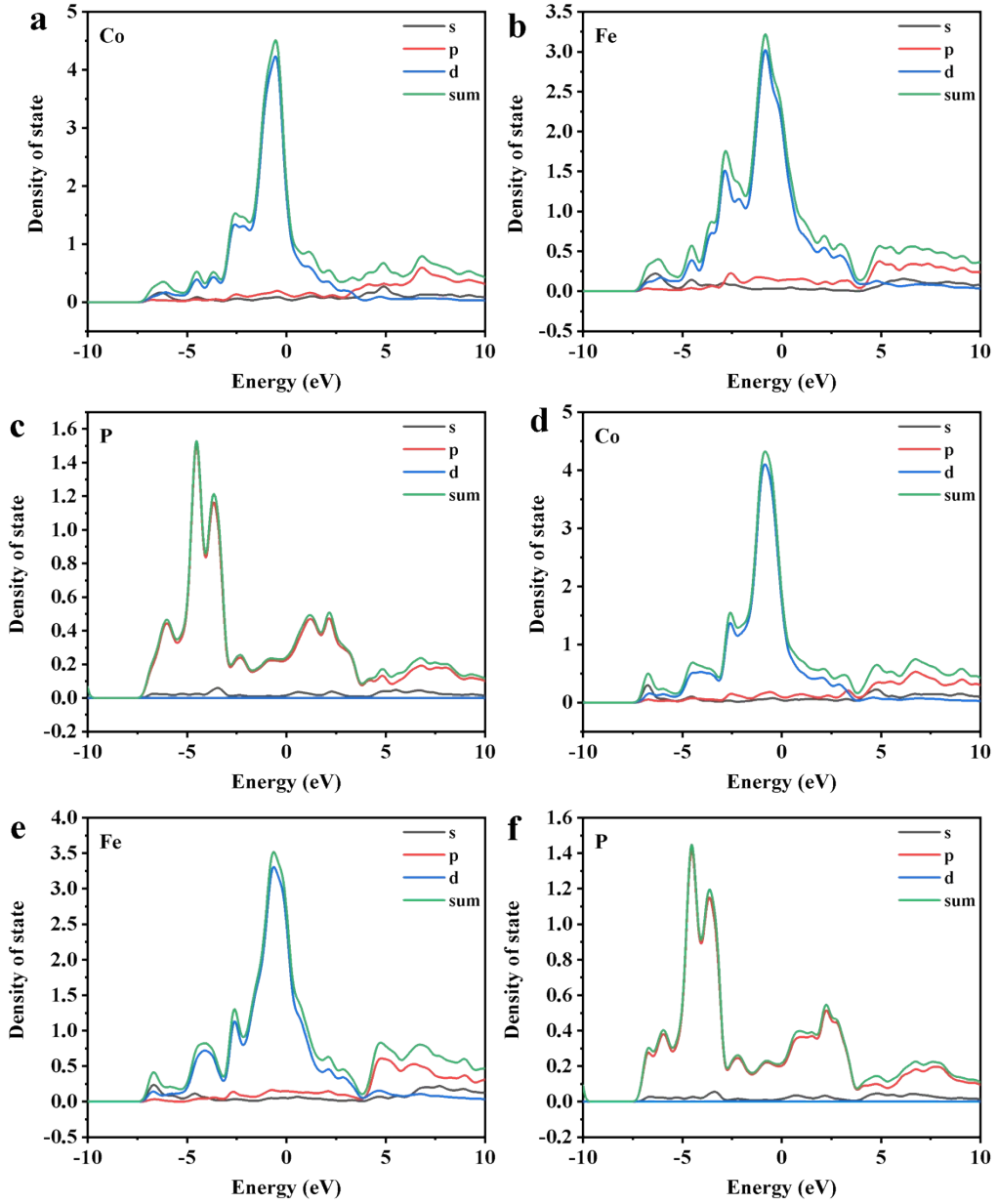

Fig. S11 The partial density of states, (a) Co , (b) Fe and (c) P for the $FeCo_2P$-$Fe_{1\text{-}Site}$; (d) Co , (e) Fe and (f) P for the $FeCo_2P$-$Fe_{2\text{-}Site}$.

Table S1 the molar amount of every atom for the $Cr_{0.1}$-$FeCo_2P$/NF catalyst.

Element	Mass fraction %	Atomic fraction %
Co	3.13	8.49
Cr	0.32	0.62
Fe	0.89	2.75
P	20.96	16.34
O	58.07	54.22
C	14.04	16.04

[1] Y. Feng, X. Wang, P. Dong, J. Li, L. Feng, J. Huang, L. Cao, L. Feng, K. Kajiyoshi, C. Wang, Boosting the activity of Prussian-blue analogue as efficient electrocatalyst for water and urea oxidation, Sci. Rep-Uk., 9 (2019) 15965.

[2] P. Babar, K. Patil, D.M. Lee, V. Karade, K. Gour, S. Pawar, J.H. Kim, Cost-effective and efficient water and urea oxidation catalysis using nickel-iron oxyhydroxide nanosheets synthesized by an ultrafast method, J. Colloid Interf. Sci., 584 (2021) 760-769.

[3] H.A. Bandal, H. Kim, In situ construction of Fe_3O_4@FeOOH for efficient electrocatalytic urea oxidation, J. Colloid Interf. Sci., 627 (2022) 1030-1038.

[4] C. Chen, L. Jin, L. Hu, T. Zhang, J. He, P. Gu, Q. Xu, J. Lu, Urea-oxidation-assisted electrochemical water splitting for hydrogen production on a bifunctional heterostructure transition

metal phosphides combining metal-organic frameworks, J. Colloid Interf. Sci., 628 (2022) 1008-1018.

[5] Y. Wu, H. Wang, J. Ren, X. Xu, X. Wang, R. Wang, Electrocatalyst based on Ni_2P nanoparticles and NiCoP nanosheets for efficient hydrogen evolution from urea wastewater, J. Colloid Interf. Sci., 608 (2022) 2932-2941.

[6] L.N. Sha, J.L. Yin, K. Ye, G. Wang, K. Zhu, K. Cheng, J. Yan, G.L. Wang, D.X. Cao, The construction of self-supported thorny leaf-like nickel-cobalt bimetal phosphides as efficient bifunctional electrocatalysts for urea electrolysis, J. Mater. Chem. A, 7 (2019) 9078-9085.

[7] H.Z. Xu, K. Ye, K. Zhu, Y.Y. Gao, J.L. Yin, J. Yan, G.L. Wang, D.X. Cao, Transforming Carnation-Shaped MOF-Ni to Ni-Fe Prussian Blue Analogue Derived Efficient Bifunctional Electrocatalyst for Urea Electrolysis, ACS Sustain. Chem. Eng., 8 (2020) 16037-16045.

[8] G.Q. Liu, C. Huang, Z.H. Yang, J.H. Su, W.X. Zhang, Ultrathin NiMn-LDH nanosheet structured electrocatalyst for enhanced electrocatalytic urea oxidation, Appl. Catal. A-Gen., 614 (2021) 118049.

[9] Y.F. Ren, C.T. Wang, W. Duan, L.H. Zhou, X.X. Pang, D.J. Wang, Y.Z. Zhen, C.M. Yang, Z.W. Gao, MoS_2/Ni_3S_2 Schottky heterojunction regulating local charge distribution for efficient urea oxidation and hydrogen evolution, J. Colloid Interf. Sci., 628 (2022) 446-455.